

Monitor Unit Calculations for External Photon and Electron Beams

AAPM Annual Meeting Refresher Course
Salt Lake City, Utah
July 25, 2001

John P. Gibbons, Jr., Ph.D.
Palmetto Richland Memorial Hospital
Columbia, South Carolina

Introduction

Based on clinical dose-response data, the ICRU states that dosimetry systems must be capable of delivering dose to an accuracy of 5%.¹ Many factors contribute to both random and systematic deviations in dose delivery, including daily patient setup, target delineation, and dose calculation. The accurate determination of dose per monitor unit (MU) at a single calculation point is an essential part of this process.

There are many methods used to determine linear accelerator MUs in the United States. In 1997, the European Society for Therapeutic Radiology and Oncology (ESTRO) published the IAEA's recommendations for photon beam calculations.² Although highly detailed, this document is limited to photon calculations on the central axis, and does not cover asymmetric fields, dynamic wedges or multileaf collimators. Furthermore, the ESTRO methodology is scarcely utilized within this country, due to its extensive use of new nomenclature and lack of formal AAPM endorsement.

In the spring of 1999, the Southeast Chapter of the American Association of Physicists in Medicine sponsored a symposium entitled "Monitor Unit Calculations for External Photon and Electron Beams." Rather than recommending a standard formalism, speakers in the two-day symposium were asked to describe the calculation method they use in a specific clinical situation. The proceedings of this symposium became the framework for the book Monitor Unit Calculations for External Photon & Electron Beams,³ published last year. This presentation will discuss the major findings of this work.

Photon Calculations

Overview

The introduction of medical linear accelerators forced the introduction of new formalisms to determine treatment time. For example, the tissue phantom ratio (TPR) introduced by Karzmark⁴ in 1965 avoided the problems inherent in the measurement of in-air quantities for high energy photon beams. As technology has added capabilities to modern linacs, additional dosimetric quantities and terms have been introduced to better determine dose per MU.

For every treatment field, the number of MUs required to deliver a specified dose D to a specified point at position (x,y) and depth d within a patient must be determined. The calculated value depends on the reference dose rate k (e.g., $k=1$ cGy/MU) of the linac at source-calibration distance, SCD . Many dosimetric quantities are dependent on field size; determined either by the

collimating jaws or by the “effective” field size incident on the patient. Although the field size may be quite irregular, it is typically approximated by a single independent variable—for example, the length of a side of a square field with equivalent dosimetry.

Perhaps the most commonly used formalism is that discussed in Chapter 10 of The Physics of Radiation Therapy⁵ by Khan. For example, using TPRs and the point of calculation located at a source-point distance SPD , MUs are given by:

$$MU = \frac{D}{k \cdot TPR(d, r_{d,eff}) \cdot S_c(r_c) \cdot S_p(r_{d,eff}) \cdot TTF \cdot OAR(x, y, d) \cdot (SCD/SPD)^2} \quad (1)$$

where S_c and S_p represent collimator and phantom scatter factors, TTF is the total transmission factor for physical (e.g., compensators, wedges, trays) and virtual (e.g., dynamic or virtual wedges) attenuators, and OAR is the off-axis ratio.

TPR is defined as the ratio of dose at a given point in phantom to the dose at the same point in the beam at a fixed reference depth. In addition to TPR , the values of S_c , S_p and TTF are affected by the choice of reference depth. The ESTRO report recommends a reference depth of 10cm to avoid contributions of electron contamination in the head. In the Khan formalism, this reference depth is chosen as the maximum depth of maximum dose. This definition is a revision of the definition of the tissue maximum ratio⁶ (TMR) and is illustrated in Figure 1. As defined, TMR is dependent on the depth d , and the “effective” field size on the patient (i.e., excluding blocked, fall-off regions, etc.), projected to that depth ($r_{d,eff}$).

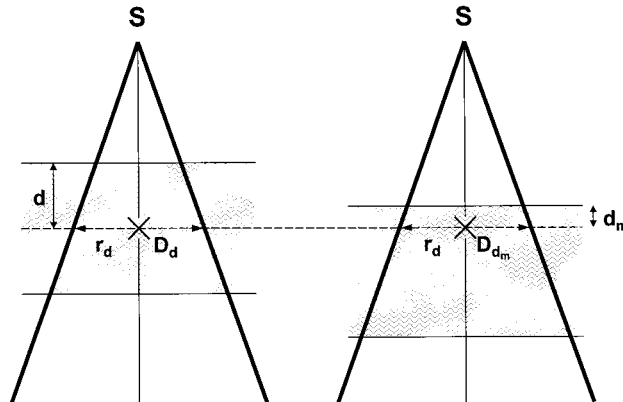


Figure 1. Diagram illustrating definition of TPR.

Regardless of the depth of normalization chosen, it is important that a consistent reference depth be utilized for all dosimetric quantities. That is, k , S_c , $S_{c,p}$, wedge and tray factors, etc., should all be measured at this depth.

At the reference depth, TMR is set to unity. At this depth, the change in dose as field size, $S_{c,p}$, is increased is mainly due to two independent effects: The change in the amount of radiation from the head of the treatment unit and the change in amount of scattered radiation from the patient. Thus this function is separated into the collimator and scatter factor factor, which depend on the collimator jaw size¹ r_c and the effective field size on the patient $r_{d,eff}$, respectively. The most common method for determining S_p is comparing measurements of the total output, $S_{c,p}$, and the collimator scatter S_c :

¹ With the notable exception of linacs equipped with upper or lower jaw replacement MLCs.

$$S_p(r) = S_{c,p}(r)/S_c(r) \quad (2)$$

Head or Collimator Scatter

The collimator scatter factor varies with several machine-dependent quantities such as flattening filter and collimator jaw location, presence and/or magnitude of jaw backscatter into monitor chamber, extent of custom blocking, etc. The collimator scatter factor may be separated into that due to monitor chamber backscatter and that due to photons scattered at some point within the head. For modern linacs, the contribution of backscatter is small, typically varying by less than 3% for all field sizes.⁷ Monte Carlo simulations⁸ and analytic methods⁹ confirm that the majority of head scattered photons originate in the flattening filter and primary collimator, with a smaller contribution arising from the adjustable jaws. Nevertheless, despite the obvious complexity of collimator scatter, several authors have shown that a radially-symmetric two dimensional extended source model is adequate in reproducing measured head scatter factors to within $\pm 1\%$.

Traditionally, S_c 's have been measured in-air using an ion chamber with build-up cap. The cap is chosen to have a thickness approximately equal to the normalization depth, d_m . It is important to completely encompass the buildup cap for all fields measured so that the scattered radiation from the cap remains constant. For higher energy photon beams, extended distances of high Z materials have been used for smaller field sizes, although discrepancies have been noted for high Z build-up caps.¹⁰ For larger depths of normalization, a cylindrical mini-phantom as suggested by van Gasteren¹¹ may be used. With the phantom aligned coaxial with the central axis of the beam, the chamber is positioned at a normalization depth of 10cm, while the radius of the phantom remains less than d_m . In either case, care must be taken to minimize competing effects, such as scatter from walls, floor, support stand, etc.

In order to determine the collimator scatter factor for intermediate or rectangular field sizes, it is usually assumed that the equivalent square relationship holds. Figure 2a demonstrates measured square and rectangular field data, using the 4A/P rule to determine the equivalent square. The rectangular field data, obtained keeping one jaw fully open and varying the other, demonstrate the collimator exchange effect: The output differs for rectangular fields when the upper and lower jaw values are interchanged. Although the magnitude of this effect is limited to around 3%, agreement can be improved if a more accurate model is used. In an extended source model, for example, the collimator scatter is dependent on the area of the scattering source (e.g., flattening filter) visible to the point of calculation. Using this "points-eye-view" model, the data is replotted in figure 2b versus the equivalent square of the flattening filter. These data are noticeably more consistent. Further improvement can be obtained if the monitor backscatter effects are removed (Fig. 2c).

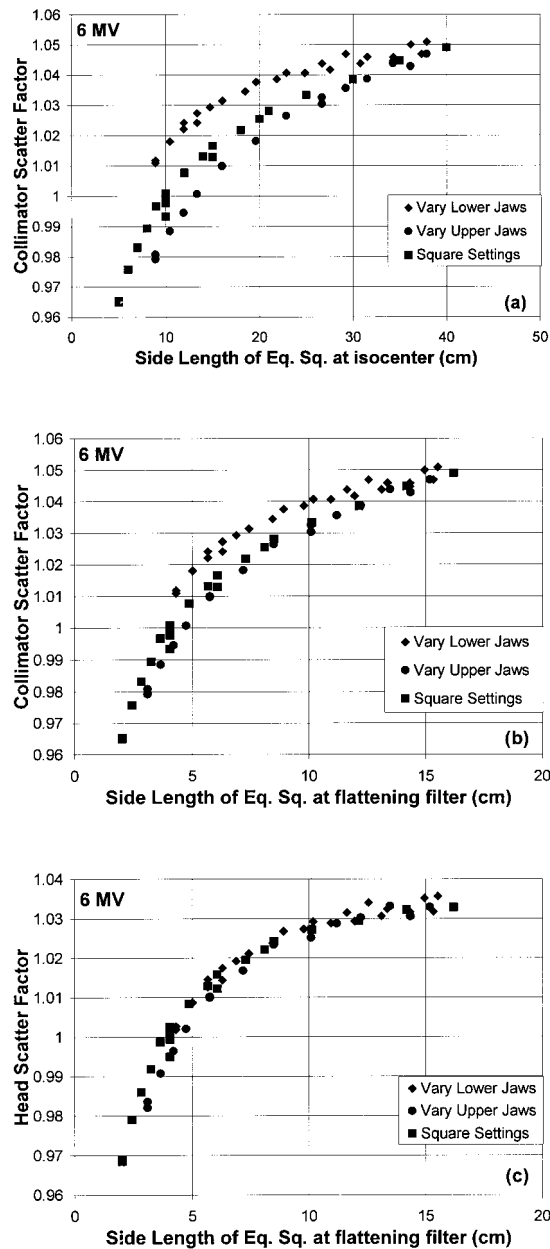


Figure 2. Illustration of collimator scatter. (a) Collimator scatter factor for square and rectangular fields. Data are normalized to field size ($4A/P$) at isocenter (b) Same data, renormalized to field size at the flattening filter, as seen from points eye view; and (c) Same as (b), with corrections for monitor chamber backscatter. Reprinted from Lam et al., *Monitor Unit Calculations with Head Scatter Factors*.³

Physical Attenuators

The introduction of external filters into the photon beam will affect the dose rate per MU at any point of calculation. Although the most direct effect is the attenuation of the primary beam within the filter, the photons scattered by the filter, both towards and away from the point

of calculation, will affect the dose calculation as well. The latter effects become more important as the thickness of the filter increases, with scatter effects usually considered only for wedges.

For blocking or shadow trays, these secondary effects are usually negligible. Since the presence of the tray will affect the build-up region through the production and absorption of secondary electrons, it is recommended that tray factors be measured at a depth beyond the maximum range of electron contamination. Consideration should also be given to the presence of mounting holes or slots.

Unlike shadow trays, compensators are specifically designed to effect the dose rate within the field. Compensator attenuation factors are required if filter material is placed over the point of calculation and may be determined by direct measurement or approximated by effective (broad-beam) linear attenuation coefficients.¹² Alternatively, compensators may be treated as replacing tissue deficit of thickness τ/ρ_e , where τ is a factor which accounts for the resulting loss of scatter due to the compensator's placement in the collimator head, and ρ_e is the electron density of the filter.

Wedge filters have been used to modify photon beams for over 50 years. Wedges may be divided into two types, defined by their placement relative to the secondary collimator jaws. Internal or motorized wedges are placed upstream of the collimating jaws and are designed using a single wedge with a large wedge angle (e.g, 60°). In contrast, external wedges are placed by hand below the collimating jaws, at source-wedge distances ranging from 40-70% of the SAD. Wedge factors can be dependent on field size, depth and SSD.

The field size dependency has been found to be greatest for internal wedges. In a survey of a number of RPC-audited facilities, Taylor concluded that a field size dependence is required if the wedge transmission factor is less than 0.65. In an attempt to quantify the magnitude of field size dependency, Heukelom proposed that the amount of scattered photons from a wedge should be proportional to both the volume of irradiated wedge, as well as the probability for photon collision within the wedge.¹³ This approach showed remarkable agreement for a number of different machines equipped with internal wedges.

The depth dependence of wedge factors generally increases with both depth and wedge angle, but is also dependent on wedge material. The mechanism for this effect has been attributed both to beam hardening and dose gradient effects.¹⁴ McCullough introduced a relative wedge factor, defined as the ratio of percent depth dose with and without a wedge. As a general rule, they found for depths less than 10 cm, no deviation over 2% is made if this quantity is ignored. Nevertheless, the increased use of wedged fields for depths beyond 10cm has increased the use of the factor in the clinic. Taylor's review concluded that depth dependency should be included if the photon energy is less than 10MV and the wedge factor is less than 0.65.

Virtual or Dynamic Wedges

As with physical wedges, filterless wedges may be accounted for using a transmission factor to describe the effect on dose per MU. In contrast to physical wedges, however, filterless wedges do not display a strong dependence with either depth or SSD. Off-axis dependencies are complex and must be handled carefully.

The current Varian implementation is entitled enhanced dynamic wedge, or EDW. EDW is oriented in the y-direction (i.e., upper jaws) only, allows seven discrete wedge angles and

asymmetric fields. The moving jaw's position versus MU is determined from a segmented treatment table (STT) which is calculated from a "golden" STT specific to that photon energy.

A number of different publications have discussed the determination of EDW transmission factors, each with varying degrees of complexity.^{15,16,17} EDW factors demonstrate a large field size dependence, varying by almost a factor two over the full range of field sizes. As the golden STT is independent of treatment machine, one may utilize a single set of transmission factors for each energy.¹⁵

The Siemens implementation, entitled virtual wedge (VW), was designed to avoid a field size dependent transmission factor. With VW, the programmed MU is equivalent to the number of MUs the central axis is unblocked by the moving jaw. The resulting TF is with 2% of 1.0 for all but large field, large angle wedges.¹⁸

Multileaf Collimators

Multileaf collimators (MLCs) have been implemented either as upper jaw replacement (Elekta), lower jaw replacement (Philips) or as tertiary collimators (Varian). MU calculations are modified by these devices in the selection of appropriate field size for the dosimetric parameters. As both TPR and S_p depend on the effective field size incident on the patient, these terms are modified to include the reduction of field size due to the use of the MLC. The collimator scatter function, S_c , however, depends on the type of MLC configuration is used.

For upper jaw replacement MLCs, Palta¹⁹ has shown that the effective area blocked by the MLC is the appropriate argument for the collimator scatter term. For lower jaw replacement, Das²⁰ demonstrated this to be true as well. As tertiary collimators, Klein found that most clinical MLC arrangements were best characterized using the collimator jaw settings to define the collimator scatter, rather than the effective MLC area. It is worth noting also that each of these studies was made for static, non-IMRT fields.

Asymmetric Field Calculations

The majority of clinical calculations are made to a point located along the central axis of the beam. In choosing off-axis calculation points, it is best to establish a new definition of the field central ray as the fanline passing through or near the geometric center of the field, with the distance off-axis defined as that projected to the machine isocenter. In addition to the changes in SSD, depth, effective field size at this point, some method for accounting for off-axis differences in primary beam intensity and energy should be employed.

A number of different techniques have been proposed to calculate dose to points off axis.^{21,22,23,24} It has been suggested that such calculations may be made using central axis dosimetry functions (TMR , S_p , etc.) and multiplying the calculated dose rate by an off-center of off-axis ratio $OAR(x,d,r)$. The function $OAR(x,d,r)$ is dependent on the off-axis distance x , depth d , as well as the effective field size at the off-axis point. The earliest recommendation was to equate $OAR(x,d,r)$ with large field profile data. However, it has been demonstrated that this approach breaks down at larger off-axis distances, since profile data contains changes in the relative scatter contribution within the phantom.²³

Both Chui and Mohan²⁵ and Gibbons and Khan²⁶ discuss the use of the primary off-axis ratio, or $POAR(x,d)$, to improve the agreement. $POAR$ may either be extracted from existing

profile data, or measured independently. In almost all cases, agreement within 2% is obtained with this factor.

Less data is available for asymmetric calculations with modifiers. In the gradient direction, Khan discussed the use of asymmetric field calculations with physical wedges, using large field wedge profile data.²⁷ In the non-gradient direction, Chui and LoSasso²⁸ noted differences in the off-axis characteristics of wedged and open fields. As with open fields, additional studies have shown improvement in both directions using off-axis changes in the primary wedged-field.²⁹

Unlike physical wedges, profiles in the non-gradient direction of dynamic wedges have shown close agreement with those from the corresponding open fields. In the gradient direction, the analytic method of Gibbons has demonstrated agreement within 2% for the determination of off-axis EDW factors.¹⁷

Heterogeneity Corrections

The use of heterogeneity corrections in dose calculations is by no means universal. Indeed, within this country several national protocols exist which require dosimetry based on the assumption of a homogenous patient. In every clinic, it is important that the physicians be made aware of the capabilities and limitations of the treatment planning system and the resultant effects this will have on patient treatment plans. The introduction of more accurate dosimetry may not be “what the doctor ordered” if it changes what they have grown accustomed to in their years of clinical experience.

It is useful to distinguish between absolute dosimetry (i.e., the dose/MU at the point of calculation) and relative dosimetry (i.e., the isodose distribution relative to the point of calculation). Heterogeneity corrections may be applied to either situation or both.

A number of heterogeneity correction methods exist in a wide range of complexity. The simplest method is to consider changes in the primary dose only. The best known of these methods is the “ratio of TARs” method, which may be implemented by using a scaled depth d' for the TPR, where

$$d' = \sum_{i=1}^n d_i x \rho_i \quad (3)$$

where ρ_i is the electron density relative to water of the i^{th} element.

Improved accuracy may be obtained with the power law TAR, or Batho method³⁰, which accounts for changes in primary and scatter radiation under assumptions of electronic equilibrium. Computed correction factors under this method are usually accurate to within 3% if the point of calculation is not in a region of electron disequilibrium.

Electron Calculations

Overview

MU calculations for electron beams are less complex than those for photon beams. The relationship between prescribed dose (to the calibration depth), D , dose output at the nominal SSD, O , and MU may be written

$$MU = \frac{D}{O(E, CS, FS) \bullet Gap Factor} \quad (4)$$

Dose output depends on the beam parameters, which includes electron energy (E), applicator or cone size (CS), and insert field size (FS). The effect of SSD on output may be incorporated into O , or separated as an independent *Gap Factor* as shown in equation 4. Typically, dose output does not depend on patient heterogeneity as the prescription point is relative to dose at a point in water.

For fixed applicators and cones, the dose output versus cone and insert field size is measured at the time of beam commissioning. For a particular energy and cone size, inserts of varying square field size will have similar outputs as long as conditions of lateral electronic equilibrium are maintained. The output for rectangular field inserts may be determined using the square root method of Mills.³¹ Depending on the degree of irregularity, many custom fields may often be approximated by rectangular fields.

The use of off-axis corrections for electron monitor units is not common. Typically, electron beams are specified to maintain flatness within a few percent of the central axis value at the depth of d_{max} . The determination of equivalent field size and SSD should be made at the off-axis point.

For machines equipped with variable collimators, Mills *et al.*,³² showed that the square root method was insufficient for rectangular field sizes. Similar to the collimator exchange effect for photons, the output for these machines was not symmetric with the changing of X and Y dimensions. They proposed a “1-D method” to correct for possible changes in output for machines with this configuration.

Irregular-Shaped Electron Fields

If the field defined by the insert is small enough, the condition of lateral scatter equilibrium (LSE) is no long fulfilled. If the field is highly irregular, special dosimetry may be required to determine the dose distribution in addition to the dose per MU at the point of calculation. Output factors may be measured with an ion chamber, diode or film, depending on the beam geometry and field size. Important requirements are that the fluence across the sensitive volume of the detector be as uniform as possible.

Khan *et al.*,³³ proposed a formalism for the determination of output factors for electron fields of any shape. The output factor is modified by a quantity entitled the lateral build-up ratio (LBR), defined as the ratio of the central axis depth dose in a circular field of radius R to that in a broad field of the same incident fluence. For arbitrary field sizes, a sector integration is made to determine the mean value of LBR for calculation.

Extended SSD Calculations

In many patients, treatments must be made at extended SSDs due to anatomical or technical limitations. A simple inverse square correction based on the nominal SSD cannot be applied to the output factors determined. Rather, any correction must account for electron scatter in the scattering foil, applicator and air. Two methods have been proposed for the incorporation of these effects into the MU formalism.

One method defines a virtual source as the origin for the divergence of the electron beam. This point may be determined in a number of ways and is utilized to determine the inverse square fall-off of the unscattered electron beam. To account for scatter in the gap, an additional air gap correction term is applied to the inverse square predicted output.

The second method defines an effective source position based on measured electron output changes with SSD. In this method the air gap correction term is avoided by applying an inverse square correction using the effective source to surface distance (SSD_{eff}) for the Gap Factor calculation. SSD_{eff} is a function of energy and field size, and is determined by measurement at the time of commissioning. Khan³⁴ has shown that SSD_{eff} is independent of depth of measurement, so that all measurements may be made at a broad beam d_{max} . Additionally, Roback has shown that for a given insert size, the size of the applicator has only a weak effect on SSD_{eff} .³⁵

Acknowledgements

The author is greatly indebted to Faiz Khan, Kwok Lam, Eric Klein, David Mellenberg, Marc Sontag, Nicholas Detorie, Kenneth Hogstrom, and Don Roback for each of their efforts in putting the book together. These faculty were chosen because of their expertise in the field, and each of their contributions have greatly enhanced the text.

¹ International Commission on Radiation Units and Measurements. Report 24. Determination of Absorbed Dose in a Patient Irradiated by Beams of X and Gamma-ray Beams in Radiotherapy Procedures, ICRU publication, Bethesda, USA 1976.

² A. Dutreix, B.E.Bjarngard, A. Bridier, B. Mijnheer, J.E. Shaw, H. Svensson: Monitor unit calculation for high energy photon beams. Physics for clinical radiotherapy Booklet No. 3. Gauant (Leuven/Apeldoorn), 1997.

³ Monitor Unit Calculations for Photon & Electron Beams. J. P. Gibbons, ed., Advanced Medical Publishing (Madison), 2000.

⁴ Karzmark, C.J., Dewbert, A., Loevinger, R. Tissue-phantom ratios – an aid to treatment planning. Br. J. Radiol. **38**, 158 1965.

⁵ Khan, F.M., The Physics of Radiation Therapy, 2nd Ed., Williams and Wilkins, Baltimore, 1994.

⁶ Holt, J.G., Laughlin, J.S., Moroney, J.P. Extension of concept of tissue-air ratios (TAR) to high energy x-ray beams. Radiology **96**, 437 1970.

⁷ Kubo, H. Telescopic measurement of backscattered radiation from secondary collimator jaws to a beam monitor chamber using a pair of slits. Med. Phys. **16**: 295-298, 1989.

⁸ Chaney EL, Cullip TJ, Gabriel TA: A Monte Carlo study of accelerator head scatter. Med Phys **21**: 1383-1390, 1994.

⁹ Ahnesjo, A. Collimator scatter in photon therapy beams. Med Phys **22**: 267-278, 1995.

¹⁰ Weber L, Nilsson P, Ahnesjo A. Build-up cap materials for measurement of photon head-scatter factors. Phys Med Biol. **42**: 1875-1886, 1997.

¹¹ Van Gasteren, J.J.M., Heukelom, S., van Kleffens, H.J., van der Laarse, R., Venselaar, J.L.M., Westermann, C.F. The determination of phantom and collimator scatter components of the output of megavoltage photon beams: measurement of the collimator scatter part with a beam co-axial narrow cylindrical phantom. Radiotherapy and Oncology **20**, 250, 1991.

¹² Bagne FR, Samsami N, Hoke SW, Bronn DG. A study of effective attenuation coefficient for calculating tissue compensator thickness. Med Phys **17**: 117-121, 1990.

¹³ Heukelom S, Lanson JH, Mijnheer BJ. Wedge factor constitutions of high energy photon beams: field size and depth dependence. Radiother Oncol **30**: 66-73.

¹⁴ Kalend AM, Wu A, Yoder V, Maitz A. Separation of dose-gradient effect from beam-hardening effect on wedge factors in photon fields. Med Phys **17**: 701-704, 1990.

¹⁵ Liu C, Palta JR. Characterizing output for the Varian enhanced dynamic wedge field. Med. Phys. **25**: 64-67, 1998.

-
- ¹⁶ Klein EE, Gerber R, Zhu XR, Oehmke F., Purdy JA. Multiple machine implementation of enhanced dynamic wedge. *Int J Rad Onc Biol Phys* **40**: 977-985, 1998.
- ¹⁷ Gibbons JP. Calculation of enhanced dynamic wedge factors for symmetric and asymmetric photon fields, *Med. Phys.* **25**: 1411-1418, 1998.
- ¹⁸ Desobry GE, Waldron TJ, Das IJ. Validation of a new virtual wedge model. *Med Phys.* **25**:71-72, 1998.
- ¹⁹ Palta JR, Yeung DK, Frouhar V. Dosimetric considerations for a multileaf collimator system. *Med Phys* **23**: 1219-1224, 1996.
- ²⁰ Das IJ, Desobry GE, McNeeley SW, Cheng CC, Schultheiss TE. Beam characteristics of a retrofitted double focused multileaf collimator. *Med Phys* **25**: 1676-1684, 1998.
- ²¹ A.G. Kepka, P.M. Johnson, and J. David, "The effect of off-axis quality changes on zero-area TAR for megavoltage beams," *Phys Med. Biol.* **30**, 589-595 (1985).
- ²² F. M. Khan, B. J. Gerbi, and F. C. Deibel, "Dosimetry of asymmetric x-ray collimators," *Med Phys* **13**, 936-941 (1986).
- ²³ D.D. Loshek and K.A. Keller, "Beam profile generator for asymmetric fields," *Med. Phys* **15**, 604-610 (1988).
- ²⁴ W. Kwa, O. Kornelsen, R.W.Harrison, and E. El-Khatib, "Dosimetry for asymmetric x-ray fields," *Med. Phys* **21**, 1599-1604 (1994).
- ²⁵ C.Chui and R. Mohan, "Off-center ratios for three-dimensional dose calculation," *Med. Phys* **13**, 409-412 (1986).
- ²⁶ J.P.Gibbons and F.M.Khan, "Calculation of dose in asymmetric photon fields," *Med Phys* **22**, 1451-1457 (1995).
- ²⁷ F.M.Khan, "Dosimetry of wedged fields with asymmetric collimation," *Med. Phys.* **20**, 1447-1451 (1993).
- ²⁸ C-S Chui and T LoSasso, "Beam profiles along the nonwedged direction for large wedged fields," *Med Phys* **21**, 1685-1690.
- ²⁹ D. Georg, "Monitor unit calculation on the beam axis of open and wedged asymmetric high-energy photon beams," *Phys. Med. Biol.* **44**, 2987-3007 (1999).
- ³⁰ Batho HF. Lung corrections in cobalt 60 beam therapy. *Canadian Association of Radiologists Journal.* **15**: 79-83 (1964).
- ³¹ M.D. Mills, K.R. Hogstrom, R.S.Fields. Prediction of electron beam output factors. *Med Phys* **9**: 60-68 (1982).
- ³² M.D. Mills, K.R.Hogstrom, R.S.Fields. Determination of electron beam output factors for the Therac 20. *Med Phys* **12**: 473-476 (1985).
- ³³ F.M.Khan, P.D.Higgins, B.Gerbi,F.C.Deibel, A. Sethi, D.N. Mihailidis. Calculation of depth dose and soe per monitor unit for irregularly shaped electron fields. *Phys Med Biol* **43**: 2741-2754 (1998).
- ³⁴ F.M.Khan, W. Sewchand, S.H.Levitt. Effect of air space on depth dose in electron beam therapy. *Radiol.* **126**, 249-251 (1978).
- ³⁵ D.M.Roback, F.M.Khan, J.P.Gibbons, A. Sethi, Effective SSD for electron beams as a function of energy and beam collimation. *Med. Phys* **22**, 2093-2095(1995).

Monitor Unit, Photon, Electron, Cancer. To cite this article. Alamgir Hossain, Dayal Chandra Roy, Samiron Kumar Saha, Nazrul Islam, Photon and Electron Beam in the Treatment of Cancer Patient Based on Monitor Unit Compilation, Cancer Research Journal. Vol. 4, No. 6, 2016, pp. 90-105. doi: 10.11648/j.crj.20160406.12. Copyright.Â Ohn P. Gibbons, John A. Antolak, David S. Followill, M. Saiful Huq, Eric E. Klein, Kwok L. Lam, Jatinder R. Palta, Donald M. Roback, Mark Reid and Faiz M. Khan â€œMonitor unit calculations for external photon and electron beams: Report of the AAPM Therapy Physics Committee Task Group No. 71â€™ Med. Phys. 41 031501 (2014). [3]. 1 for External Photon and Electron Beams AAPM Annual Meeting Refresher Course Salt Lake City, Utah July 25, 2001 John P., Jr., Ph.D. Palmetto Richland Memorial Hospital Columbia, South Carolina Introduction Based on clinical dose-response data, the ICRU states that dosimetry systems must be capable of delivering dose to an accuracy of 5%. 1 Many factors contribute to both random and.Â The proceedings of this symposium became the framework for the book Monitor Unit Calculations for External Photon & Electron Beams, 3 published last year. This presentation will discuss the major findings of this work. Photon Calculations Overview The introduction of medical linear accelerators forced the introduction of new formalisms to determine treatment time. @inproceedings{Gibbons2002MonitorUC, title={Monitor Unit Calculations for External Photon and Electron Beams}, author={John P. Gibbons and Chester Stanley Reft}, year={2002} }. John P. Gibbons, Chester Stanley Reft. Published 2002. Physics. Based on clinical dose-response data, the ICRU states that dosimetry systems must be capable of delivering dose to an accuracy of 5%. Many factors contribute to both random and systematic deviations in dose delivery, including daily patient setup, target delineation, and dose calculation. The accurate determination of dose per monitor unit (MU) at a single calculation